Research Article Open Access

Beyhan Erdem*, Sezer Erdem, Ramis Mustafa Öksüzoğlu

Catalytic Applications of Large Pore Sulfonic Acid-Functionalized SBA-15 Mesoporous Silica for Esterification

https://doi.org/10.1515/chem-2018-0132
received January 30, 2018; accepted August 19, 2018.

Abstract: We report the preparation of pore expanded and sulfonic acid functionalized mesoporous silica catalysts by using different kinds of swelling agents such as 1,3,5-trimethyl benzene (TMB), n-decane (D), n-tridecane (TD), and n-hexadecane (HD) at two different ratios of swelling agent/ surfactant. Non-swelled mesoporous silica catalyst, SBA-15-SO_3H, was also prepared for comparison. The performance of the sulfonic acid functionalized solid acid catalysts by using one-pot synthesis procedure was evaluated in terms of their catalytic activity in the esterification of propionic acid with methanol. The catalysts have been characterized by X-ray diffraction to investigate the phase transition between the hexagonally packed arrangement of cylindrical pores and mesocellular silica foams (MCF), and N_2 adsorption/desorption technique in terms of pore size and distributions. It was concluded from the XRD and N_2 adsorption/desorption analyses that hexagonally packed and cylindrical pore structure is maintained only for low ratio of swelling agent/surfactant and the increase of the dimension of a template micelle is accompanied by an increase in structural disruption, which was attributed to the phase transition from highly ordered hexagonal arrangement to mesocellular foam (MCF) phase with large nodded pore structures rather than cylindrical pores. Among the different swelling agents, TMB and D were found to be effective for the increase in pore diameter (up to 8 and 7.8 nm), whereas, TD and HD (6.6 nm) are effective to maintain the ordered X-ray diffraction patterns resulting mesoporous materials without giving enlargement of pore diameter in comparison with TMB and D. Pore expanded catalysts, SBA-15-SO_3H-TMB-0.1 and SBA-15-SO_3H-D-0.1, exhibit 68 and 43% enhancement in turnover frequency toward propionic acid methanol esterification, respectively, over non-swelled SBA-15-SO_3H, despite possessing similar acid strengths. The increased activity especially for SBA-15-SO_3H-TMB-0.1 and SBA-15-SO_3H-D-0.1 likely reflects the accessibility to the active sulfonic acid sites as well as acidity.

Keywords: SBA-15; Sulfonic acid; Auxiliary chemical; Functionalization.

PACS: 61.43.Gt, 81.05.Lg, 82.65.+r.

1 Introduction

Silica materials having well-organized structure of uniform pores the diameters of which are bigger than microporous zeolite's and smaller than macroporous silica gel's has stimulated considerable interest in new synthesis procedures and possible applications [1]. The need of stable materials with well-defined pores between the microporous (< 2 nm) and macroporous (> 50 nm) scale was fulfilled with the discovery of the M41S materials by Mobil researchers in 1992 [2]. The synthesis of mesoporous materials consists of the preparation of micelles in aqueous solution, the polycondensation of the inorganic silica source, and the removal of surfactants from the pores of materials. The size of formed micelles determines the pore size of final mesoporous materials [3]. Normally, a mesoporous silica material, known as SBA-15, has been developed by using polymer templated syntheses utilizing poly(ethylene oxide)-poly(propylene oxide)-poly(ethylene oxide) (PEO_{20}-PPO_{70}-PEO_{20}) triblock copolymer (Pluronic-123) as surfactant and tetraethyl ortosilicate (TEOS) as the silica source. The amphiphilic Pluronic-123 has both hydrophilic PEO and hydrophobic PPO chains and so can form aggregates in aqueous environment. The processes that occur in aqueous

***Corresponding author: Beyhan Erdem,** Uludag University, Chemistry Department, Bursa-Turkey, E-mail: gbeyhan@uludag.edu.tr
Sezer Erdem: Uludag University, Physics Department, Bursa-Turkey
Ramis Mustafa Öksüzoğlu: Anadolu University, Materials Science and Engineering Department, Eskisehir-Turkey

solution are: (1) the formation of micelles, and (2) the interaction between water molecules and PEO moiety via hydrogen bonds. The silicate source (TEOS) is hydrolyzed in aqueous solution and polymerizes to form a silica network. In SBA-15, micelles take the elongated shape accompanied by the condensation of the silica source. The building of the silica walls and the arranging of micellar rods in a hexagonal pattern occur simultaneously. That is: on one hand silica precursor is polymerized on the PEO chains, on the other hand, the decreased water content results in a reduced curvature of the micelle [4].

Highly ordered hexagonal phased SBA-15 possesses large specific surface area, large pore volume and thick pore wall, which allow hydrothermal stability. Moreover, it has abundant surface silanol groups, so organofunctionalization not only modifies the surface properties of mesoporous silica by means of silanol groups but also gives activity for catalytic applications. The direct modification process, named as one-pot method, takes place in which a tetraalkoxysilane (TEOS) condensates together with trialkoxyorganosilane precursors (3-mercaptopropyl trimethoxysilane, MPTMS, in this study) in a templating environment. The TEOS is responsible for creating the mesoporous silicate framework, while the MPTMS is related to functionalization [5]. However, its small pores may restrict the mass transfer due to the long diffusion paths [6]. The size of the pores of silica molecular sieves can be adjusted by changing the tail length of the surfactant, the templating polymers, organic additives, and also by the hydrothermal treatment conditions. According to the literature [7], the use of organic auxiliary chemicals during the synthesis process is the most efficient way to attain mesoporous material with larger pore diameter. However, further increase is limited by a phase transition from ordered hexagonal pores to disordered mesocellular foams [8]. The previous reports about catalytic applications of expanded mesopore catalysts are limited. Kato et al [9], prepared SBA-1 using only the triblock copolymer (Pluronic 123) and silica source (TEOS) and its derivatives (SBA-2 and SBA-3) using n-decane and trimethylbenzene for expanding the pore diameter in addition to Pluronic-123 and TEOS and then immobilized cytochrome c on these mesoporous silicates and obtained enhanced catalytic activity depending on pore expanding. Wilson et al [10], firstly prepared pore-expanded and sulfonic acid grafted SBA-15 over the range 6-14 nm for biodiesel production.

In this study, the swelling agents are introduced during the self-assembling process in order to increase the pore diameter of the inorganic silica benefitted from preferential solubilization of the additive in the micelle core. 1,3,5-trimethyl benzene and higher alkanes (n-decane, n-tridecane and n-hexadecane) have been used to swell the pores of SBA-15 and pore-expanded silicas were simultaneously functionalized with MPTMS followed by oxidation with H_2O_2 to achieve sulfonic acid sites by using one-pot procedure for the first time. The obtained non-swelled SBA-15-SO_3H and swelled with TMB, D, TD and HD at two different mass ratios of 0.1 and 0.5 (organic auxiliary/Pluronic-123) catalysts were tested for their catalytic performances in the esterification of propionic acid with methanol to identify the impact of pore diameter.

2 Experimental

2.1 Catalysts Preparation

In a typical synthesis, 4 g of Pluronic-123 triblock copolymer (Aldrich) was dissolved in 125 mL of 1.9 M HCl at 40°C. After completely dissolution, 0.4 and 2 g of organic auxiliary chemicals (TMB, Sigma Aldrich; D, TD, and HD, Merck) corresponding to the mass ratio of 0.1 and 0.5 for TMB/P, D/P, TD/P and HD/P, respectively, were added and left to stabilize under stirring for one hour prior to addition of 7.7 g of TEOS (Merck). Before the addition of MPTMS (0.81 g, Aldrich) and H_2O_2 (8.37 g, Merck), the mixtures were stirred for an additional an hour, followed by stirring at 40°C for 24 h. The mixtures were allowed to be gelating by aging them at 100°C for another 24 h. In direct functionalization method [11], since organic functionalities are direct components of the silica matrix, pore blocking is not a problem and organic units generally more homogeneously distributed than in materials synthesized with the grafting process. However, there are some disadvantages about direct functionalization, that is: the degree of mesoscopic order decreases with the increasing concentration of trialkoxyorganosilane due to the homocondensation instead of condensation with silica precursor and care must be taken not to destroy the organic functionality during the removal of the surfactant, which is why commonly only extractive methods can be used, and calcination is not suitable in most cases. For this reason, the surfactant and the micelle expanders were removed by refluxing the materials in 90:10% (v/v) ethanol/HCl mixture for 24 h.

2.2 Catalysts Characterization

The sulfonic acid functionalized and pore expanded materials were characterized with XRD, N_2-adsorption/desorption and FT-IR techniques. Low angle-XRD patterns were collected using a Bruker 4-circle diffractometer equipped with a Cu sealed tube point source and a Gobel Mirror optic to generate a 2D-collimated parallel beam (divergence ca. 0.03 and a lateral length of 18 mm) and an anti-scatter slit to remove background. Typically, the data were collected from 0.7 to 2° (2θ) at 40 kV and 40 mA. Nitrogen sorption isotherms were measured at 77 K with Quantachrome, Autosorb 1C sorption analyzer. Before the measurements, the samples were degassed at 200°C in vacuum for 5 h. Surface areas were calculated using the Brunauer–Emmet–Teller (BET) method over the range p/p^o = 0.03–0.2, where a linear relationship is maintained. Pore size distributions were calculated using the Barrett–Joyner–Halenda (BJH) method applied to the desorption branch of the isotherm. FT-IR measurements were performed using Perkin Elmer-UATR Two series infrared spectroscopy. The acid exchange capacities of the non-swelled SBA-15–SO_3H and swelled with TMB, D, TD, and HD at two different mass ratio of 0.1 and 0.5 (organic auxiliary/Pluronic-123) named as SBA-15-SO_3H, SBA-15-SO_3H-TMB-0.1 and SBA-15-SO_3H-TMB-0.5, SBA-15-SO_3H-D-0.1 and SBA-15-SO_3H-D-0.5, SBA-15-SO_3H-TD-0.1 and SBA-15-SO_3H-TD-0.5, SBA-15-SO_3H-HD-0.1 and SBA-15-SO_3H-HD-0.5, respectively, were measured by means of titration, using sodium chloride as exchange agent. In a typical experiment, 0.05 g of solid acid catalyst was added to 10 g of aqueous solution of sodium chloride (2 M). The resulting suspension was allowed to equilibrate and thereafter titrated potentiometrically by dropwise addition of 0.01 N NaOH (aq).

2.3 Catalytic Test

The esterification of propionic acid with methanol was carried out in an isothermal glass reactor equipped with a heating jacket the temperature of which was controlled within ±0.1°C. Stoichiometric ratio of propionic acid to methanol was (1:4) in the experiments performed at 333 K. 1,4-dioxane was used as solvent in all experiments. In a typical run, catalyst (about 0.5 g), methanol and dioxane of known amount were charged into the reactor and preheated to the reaction temperature and the esterification was commenced by adding preheated propionic acid into the mixture. The total liquid volume was 100 mL. Samples were withdrawn from reactor medium at certain time intervals and then analyzed by titration with 0.1 M sodium hydroxide to determine the amount of unreacted acid.

Ethical approval: The conducted research is not related to either human or animal use.

3 Results and Discussion

The typical small angle XRD profile for SBA-15-SO_3H is illustrated in Figure 1. The non-swelled SBA-15-SO_3H showed the strong (100) peak and very weak (110) and (200) signals (shown in inset of Figure 1), which demonstrates 2D hexagonal mesoscopic organization. The one step control of the co-condensation of TEOS and oxidation of mercapto groups in the presence of hydrogen peroxide was the major challenge in one-pot procedure and the peaks corresponding to (110) and (200) diffractions disappear in the patterns of the acid catalyst because of the introduction of MPTMS and H_2O_2 [12]. Organosilane precursor (MPTMS) fraction in the reaction mixture may decrease the degree of mesoscopic order of the SBA-15-SO_3H, because the organosilane component exhibits a disrupting effect on the structural integrity of the templating mesophase [13].

When examining the Figure 2, only the weak shoulder peak was observed at smaller scattering angle for the SBA-15-SO_3H-TMB-0.1, and no scattering signals were detectable for the SBA-15-SO_3H-TMB-0.5. This observation shows less organized pore structure of the SBA-15-SO_3H-TMB-0.5 (Figure 2a). A slight shift of the (100) diffraction peaks to lower angles indicates the increasing of the pore size of SBA-15-SO_3H. The d spacing reflected by intense (100) peaks and corresponding unit-cell parameters (a_{100}) are listed in Table 1. When TMB is added to a SBA-15-SO_3H system, the hexagonally packed pore structure is maintained only for low ratio of TMB/0.1. Upon increasing the ratio to 0.5, unfortunately, the increase of the dimension of a template micelle is accompanied by an increase in structural disruption. It was concluded from the XRD results that the increasing TMB/Pluronic-123 ratio results in phase transition from highly ordered hexagonal arrangement to mesocellular foam (MCF) phase with large nodded pore structures rather than cylindrical pores [2]. The similar results have also been found for SBA-15-SO_3H-D-0.1 and SBA-15-SO_3H-D-0.5 samples (Figure 2b). On the other hand, d_{100} shift was only found for tridecane with high ratio, SBA-15-SO_3H-TD-0.5 (Figure 2c). There has been no change in the location of the peaks for both 0.1 and 0.5 ratio samples of hexadecane, SBA-15-SO_3H-HD-0.1 and SBA-15-SO_3H-HD-0.5 (Figure 2d). Since

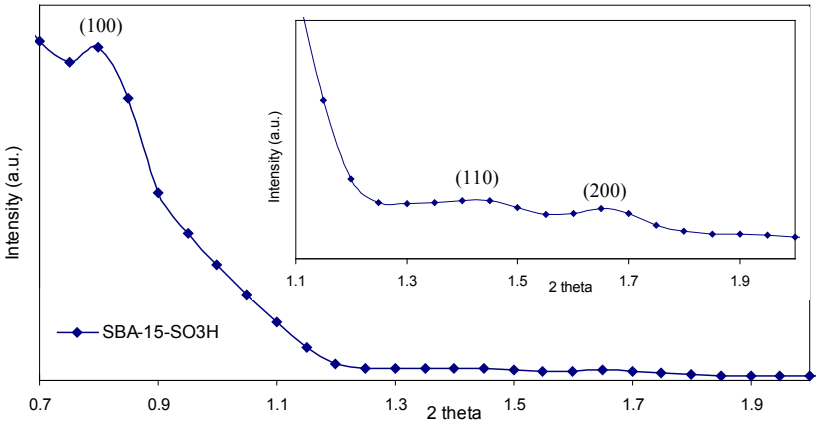

Figure 1: XRD patterns of non-swelled SBA-15-SO_3H between 0.7 and 2.0° (between 1.1 and 2.0° is in inset).

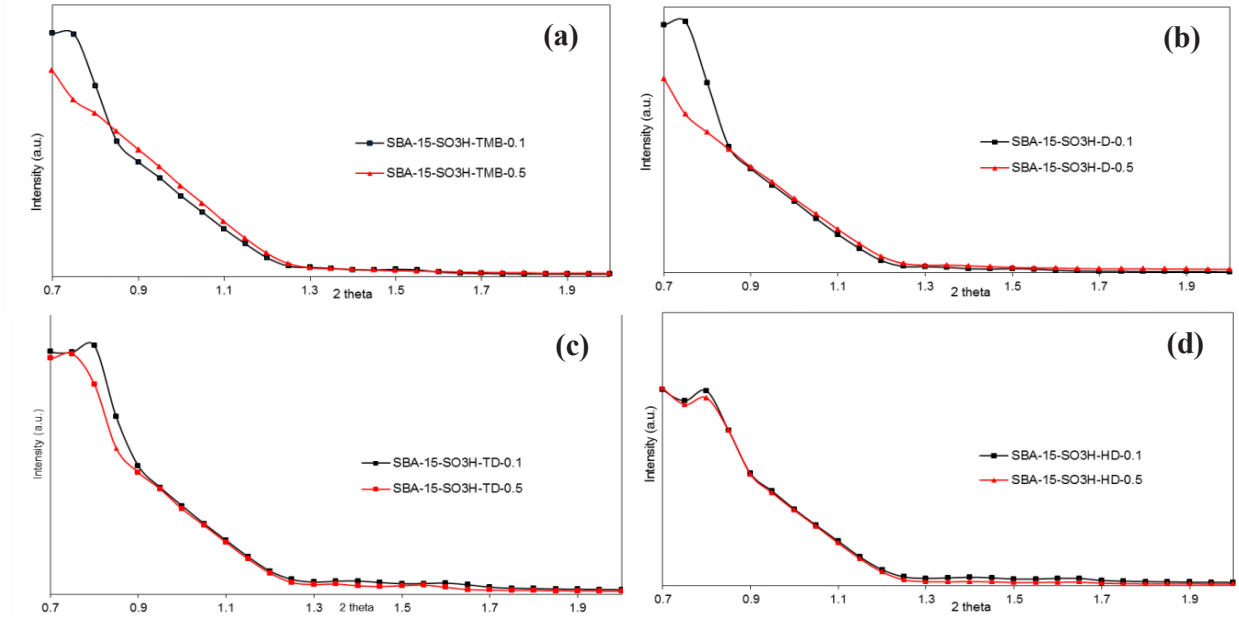

Figure 2: XRD patterns of SBA-15-SO_3H-TMB-0.1 and SBA-15-SO_3H-TMB-0.5 (a), SBA-15-SO_3H-D-0.1 and SBA-15-SO_3H-D-0.5 (b), SBA-15-SO_3H-TD-0.1 and SBA-15-SO_3H-TD-0.5 (c), SBA-15-SO_3H-HD-0.1 and SBA-15-SO_3H-HD-0.5 (d).

the solubilization of alkanes in the PPO parts leads to the swelling of the hydrophobic cores [14], towards from decane to hexadecane (as the molecular chain length increases) solubility decreases, swelling is nor successful and it is not possible to find a change in the XRD spectrum.

The N_2 adsorption/desorption isotherm and pore size distribution shown in Figure 3 reveal that bare (or non-swelled) SBA-15-SO_3H has typical Type IV isotherm and H1 hysteresis which are evidence of mesoporous silica having hexagonal arranged cylindrical pores. According to Figure 4a, SBA-15-SO_3H-TMB-0.1 has the same isotherm type of the non-swelled silica, which remains Type IV. The keeping of the cylindrical, parallel pore channels can be proved from upright step and narrow hysteresis loops in the adsorption/desorption branches. It could be detected from BJH analysis on the desorption branch that pore diameters were able to enlarged up to 8 nm by using this ratio of TMB (Table 1). The nitrogen sorption measurements show that the materials differ not only by the size of their pores but also by the pore geometry. The hysteresis loop in the isotherm of the material prepared with TMB-0.1 is of type H1, indicating the cylindrical pore

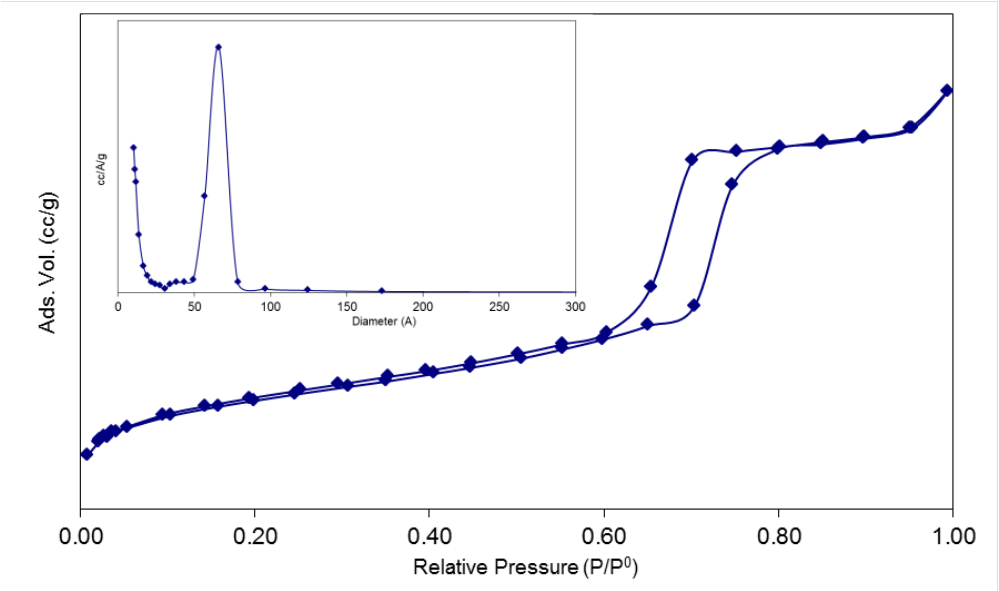

Figure 3: N_2-sorption isotherm and pore size distribution (inset) of SBA-15-SO_3H.

Table 1: The structural properties calculated by XRD and N_2 sorption results.

Samples	d_{100} (nm)[a]	a_{100} (nm)[b]	d_{pore} (nm)[c]
SBA-15-SO_3H	*11.03*	*12.74*	*6.6*
SBA-15-SO_3H-TMB-0.1	11.77	13.59	8.0
SBA-15-SO_3H-TMB-0.5	13.58	15.68	6.6
SBA-15-SO_3H-D-0.1	11.77	13.59	7.8
SBA-15-SO_3H-D-0.5	13.58	15.68	7.9
SBA-15-SO_3H-TD-0.1	11.03	12.74	6.6
SBA-15-SO_3H-TD-0.5	11.77	13.59	6.6
SBA-15-SO_3H-HD-0.1	11.03	12.74	6.6
SBA-15-SO_3H-HD-0.5	11.03	12.74	6.6

[a]calculated by $n\lambda=2d\sin\theta$, [b]calculated by $2d_{100}/\sqrt{3}$, [c]determined by peak of BJH curves.

geometry. When we increase the ratio of TMB/P from 0.1 to 0.5 the hysteresis loop is more of type H2. According to the literature [15], this indicates just as the MCF material's pore geometry which has larger compartments interconnected by smaller windows. Considering of spherical pore geometry would be more suitable for analyzing the pore size distribution of this material. Nevertheless, cylindrical pore geometry was assumed for all calculations, to make the comparison easy and to give a measurement for the non-cylindrical character of the pores in these materials. The average pore diameters calculated from the peaks of the curves, however, independent of the assumed pore geometry and are therefore correct for all materials [16].

Figure 4b shows the N_2 adsorption/desorption isotherm and pore size distribution of SBA-15-SO_3H-D-0.1 and SBA-15-SO_3H-D-0.5 samples. Similarly to the TMB swelled samples, while the isotherm and the hysteresis types are maintained at low ratio, there are not highly protected at high ratio. This pore-expansion reveals little ordered periodic mesostructures compared with TMB, with pore diameters of 7.8 nm. The swelling process with tridecane and hexadecane maintain the hexagonally packed structure of the cylindrical pores in SBA-15-SO_3H, however, they cannot increase the pore diameters. Because the solubility decreases as the chain length of the higher alkanes increases, and when we remove the surfactant together with swelling agent from the mesoporous silica, there are no structural change (Figures 4c and 4d).

According to the N_2 adsorption/desorption results, as the ratio of swelling agent to surfactant increases, the BET surface area of the swelled materials with TMB, D, TD and HD decreased, in company with an increase in mesopore volume, and also pore-expansion, matching well with the geometric changes of the mesopore network (Table 2).

All FT-IR spectra, which are shown in Figure 5, are characterized by the typical bands of mesoporous silica, such as the asymmetric stretching vibrations of Si-O-Si at 1120-1020 cm^{-1}, and symmetric stretching vibrations of Si-O-Si around 800 cm^{-1}. The band at 951 cm^{-1} corresponds to symmetric stretching vibration of Si-OH and 1630

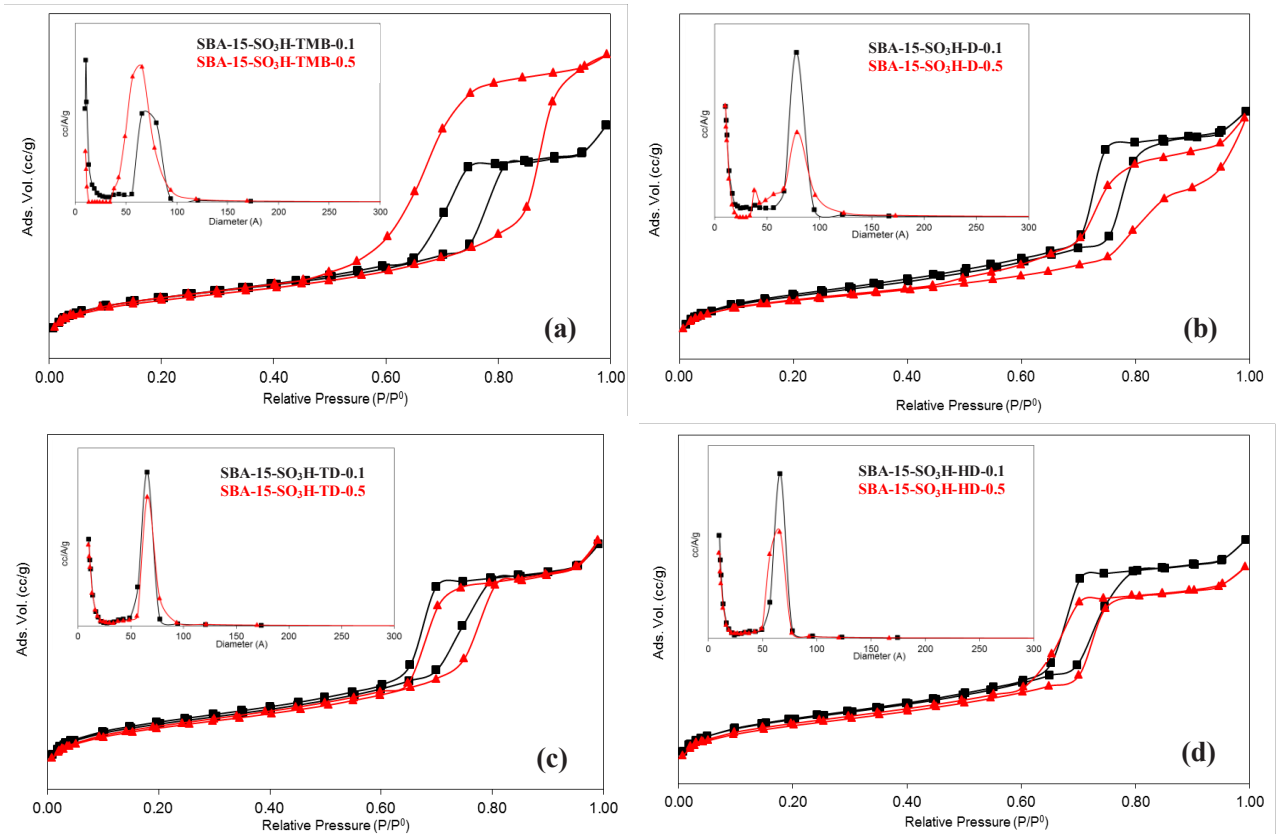

Figure 4: **(a)** N_2-sorption isotherms and pore size distributions (inset) of SBA-15-SO_3H-TMB. **(b)** N_2-sorption isotherms and pore size distributions (inset) of SBA-15-SO_3H-D. **(c)** N_2-sorption isotherms and pore size distributions (inset) of SBA-15-SO_3H-TD. **(d)** N_2-sorption isotherms and pore size distributions (inset) of SBA-15-SO_3H-HD.

Table 2: The structural (from BET/BJH analysis) and acidic properties of the samples.

Samples	S_{BET} (m^2/g)	V_{pore} (cm^3/g)	Acid Capacity (mmol H^+/g)
SBA-15-SO_3H	*627*	*1.12*	*0.8105 ± 0.0097*
SBA-15-SO_3H-TMB-0.1	620	1.14	0.8924 ± 0.0005
SBA-15-SO_3H-TMB-0.5	595	1.53	0.7941 ± 0.0219
SBA-15-SO_3H-D-0.1	645	1.19	0.9863 ± 0.0120
SBA-15-SO_3H-D-0.5	590	1.13	0.9343 ± 0.1013
SBA-15-SO_3H-TD-0.1	652	1.14	0.8894 ± 0.0172
SBA-15-SO_3H-TD-0.5	616	1.16	0.8673 ± 0.0392
SBA-15-SO_3H-HD-0.1	655	1.17	0.9526 ± 0.0445
SBA-15-SO_3H-HD-0.5	595	1.03	0.9151 ± 0.0361

cm^{-1} relates to the O-H bending vibration of water. The broad band between 3400 and 3500 cm^{-1} also appears in the FT-IR spectra of the samples, which refers to Si-OH on the surface [17,18]. S=O asymmetric-stretching (SO_2) vibrational mode at 1348 cm^{-1} assigning to SO_3H groups and the S-OH stretching vibration of SO_3H groups around 840 cm^{-1} overlapping with symmetric stretching vibrations of Si-O-Si band were observed for all sulfonic acid functionalized mesoporous silica samples [19].

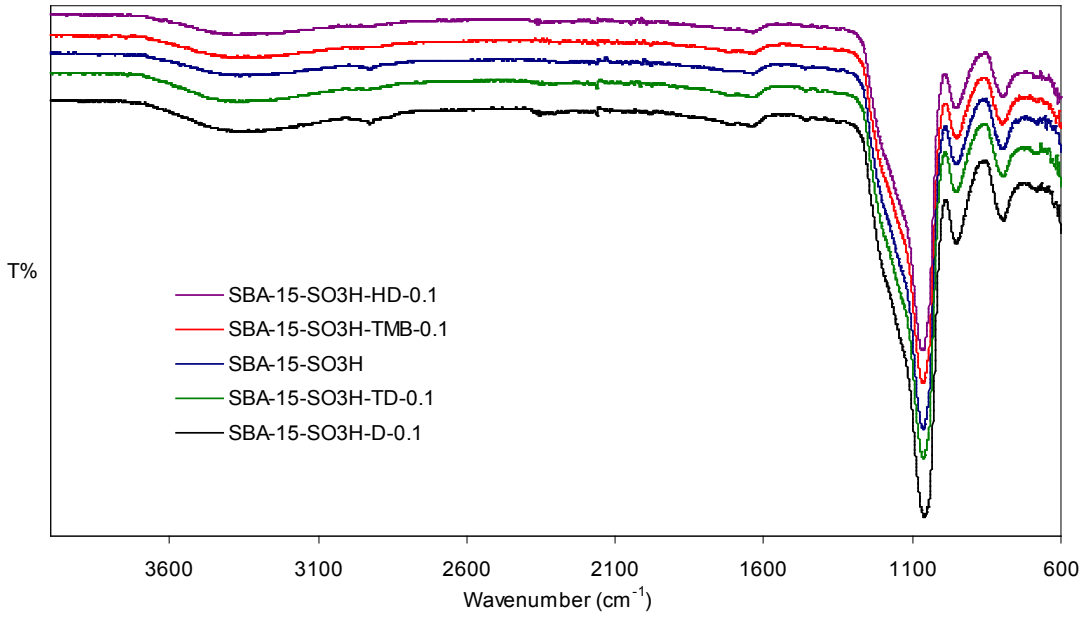

Figure 5: FT-IR spectra of non-swelled (SBA-15-SO_3H) and swelled samples.

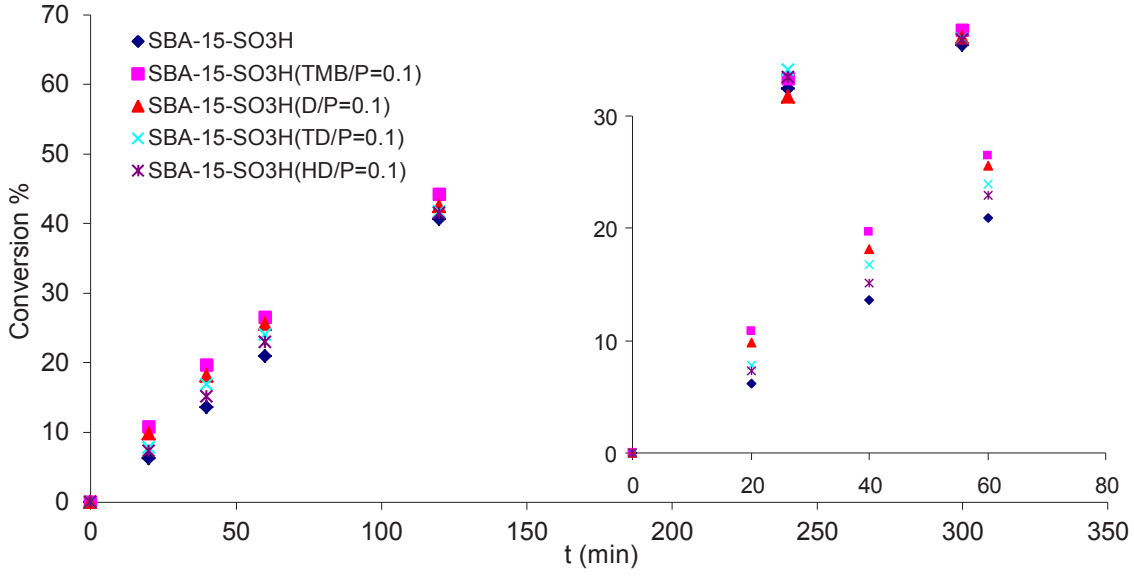

Figure 6: Conversion of propionic acid versus time (propionic acid/ methanol molar ratio: 1/1, stirring rate: 500 rpm, temperature: 60°C, catalyst: 0.5 g, solvent: 1,4-dioxane)-(early stage of reaction is given in inset).

The performance of the pore enlarged and sulfonic acid functionalized silica catalysts were tested in the esterification of propionic acid with methanol and were benchmarked against bare SBA-15-SO_3H with respect to conversion % of propionic acid (Figure 6). Although all catalysts seem to have the same activity, the enhancement is clearly seen in early stages of the esterification reaction as shown in inset of Figure 6. The corresponding Turnover Frequencies (TOFs, initial rates for the 20th minutes normalized per acid site) indicates that all pore-expanded catalysts outperform bare SBA-15-SO_3H.

According to the experimental data shown in Table 3, pore expanded catalysts, SBA-15-SO_3H-TMB-0.1 and SBA-15-SO_3H-D-0.1, exhibit 68 and 43% enhancement in turnover frequency toward propionic acid methanol esterification, respectively, over bare SBA-15-SO_3H. We attributed the

Table 3: Comparison of non-swelled SBA-15-SO_3H catalyst with related solid acids for propionic acid methanol esterification.

Catalyst	Pore diameter[a] (nm)	Conversion[b] (%)	TOF[c] (h^{-1})	Acid capacity (mmol/g)
SBA-15-SO_3H	6.6	6.2	0.4249	0.8105
SBA-15-SO_3H-TMB-0.1	8.0	10.8	0.7133	0.8924
SBA-15-SO_3H-D-0.1	7.8	9.8	0.6070	0.9863
SBA-15-SO_3H-TD-0.1	6.6	7.8	0.5264	0.8894
SBA-15-SO_3H-HD-0.1	6.6	7.3	0.4489	0.9526

[a]Determined by peak of BJH curves. [b]Conversion after 20 min reaction time. [c]Initial reaction rates per acid capacity for 20 min reaction time.

improved performance to the greater accessibility of sulfonic acid sites caused by larger mesopores. On the other hand, acid capacity is another factor influencing the activity of the reaction [20]. It is therefore interesting to note the similarities in acid capacity values, which likely means similar acid strength of the catalysts. According to the enhancing in the conversions of the reaction, the increased activity especially for SBA-15-SO_3H-TMB-0.1 and SBA-15-SO_3H-D-0.1 likely reflects the accessibility to the active sulfonic acid sites as well as acidity.

4 Conclusion

The pore-expanded SBA-15-SO_3H acid catalysts have been synthesized with the addition of TMB, D, TD, and HD swelling agents by using the one-pot modification method for the first time and applied to the esterification of propionic acid with methanol. As the ratio of swelling agent increases from 0.1 to 0.5, it can be concluded from nitrogen physisorption and XRD results that these materials could have ordered mesopores, but at the same time no clear long-range order could be identified. This is because mesocellular foam (MCF) phase with large nodded pore structures occur rather than cylindrical pores. Pore expansion over the range 7.8 - 8 nm for TMB and D confers an activity enhancement towards methyl propionate synthesis, attributed to the greater accessibility of sulfonic acid sites resulting from larger mesopores. In pore expanded mesoporous silica catalysts prepared by using swelling agent, pore expanding is accompanied by geometrical change. Therefore, the catalytic performance in esterification reaction depends on both the pore size and acidity of the catalyst.

Acknowledgment: This work was supported by The Commission of Scientific Research Projects of Uludag University, Project number: OUAP(F)-2015/21.

Conflict of interest: Authors declare no conflict of interest.

References

[1] Derylo-Marczewska A., Marczewski A.W., Skrzypek I., Pikus S., Kozak M., Effect of addition of pore expanding agent on changes of structure characteristics of ordered mesoporous silicas, Appl. Surf. Sci., 2008, 255, 2851-2858.
[2] Lettow J.S., Han Y.J., Schmidt-Winkel P., Yang P., Zhao D., Stucky G.D., et al., Hexagonal to Mesocellular Foam Phase Transition in Polymer-Templated Mesoporous Silicas, Langmuir, 2000, 16, 8291-8295.
[3] Blin J.L., Otjacques C., Herrier G., Su B.L., Pore Size Engineering of Mesoporous Silicas Using Decane as Expander, Langmuir, 2000, 16, 4229-4236.
[4] Fonseca-Correa R.A., Murillo-Acevedo Y.S., Giraldo-Gutierrez L., Moreno-Pirajan J.C., Microporous and Mesoporous Materials in Decontamination of Water Process, In: Dariani R.S. (Ed.), Microporous and Mesoporous Materials, InTech Open, Chapter 7, 2016.
[5] Srinivas D., Saikia L., Functionalized SBA-15 and its Catalytic Applications in Selective Organic Transformations, Catal. Surv. Asia, 2008, 12, 114-130.
[6] Xing S., Lv P., Fu J., Wang J., Fan P., Yang L., et al., Direct synthesis and characterization of pore-broadened Al-SBA-15, Micro. Meso. Mater., 2017, 239, 316-327.
[7] Jana S.K., Nishida R., Shindo K., Kugita T., Namba S., Pore size control of mesoporous molecular sieves using different organic auxiliary chemicals, Micro. Meso. Mater., 2004, 68, 133-142.
[8] Johansson E.M., Ballem M.A., Cordoba J.M., Oden M., Rapid Synthesis of SBA-15 Rods with Variable Lengths, Widths, and Tunable Large Pores, Langmuir, 2011, 27, 4994-4999.
[9] Kato K., Suzuki M., Tanemura M., Saito T., Preparation and catalytic evaluation of cytochrome c immobilized on mesoporous silica materials, J. Ceram. Soc. Jpn., 2010, 118, 410-416.
[10] Dacquin J.P., Lee A.F., Pirez C., Wilson K., Pore-expanded SBA-15 sulfonic acid silicas for biodiesel synthesis, Chem. Commun., 2012, 48, 212-214.

[11] Hoffmann F., Cornelius M., Morell J., Fröba M., Silica-Based Mesoporous Organic-Inorganic Hybrid Materials, Angew. Chem. Int. Ed., 2006, 45, 3216-3251.
[12] Lai D., Deng L., Guo Q., Fu Y., Hydrolysis of biomass by magnetic solid acid, Energy Environ. Sci., 2011, 4, 3552-3557.
[13] Hoffmann F., Fröba M., Vitalising porous inorganic silica networks with organic functions-PMOs and related hybrid materials, Chem. Soc. Rev., 2011, 40, 608-620.
[14] Sun J., Zhang H., Ma D., Chen Y., Bao X., Klein-Hoffmann A., et al., Alkanes-assisted low temperature formation of highly ordered SBA-15 with large cylindrical mesopores, Chem. Commun., 2005, 42, 5343-5345.
[15] Lukens Jr. W.W., Schmidt-Winkel P., Zhao D., Feng J., Stucky G.D., Evaluating Pore Sizes in Mesoporous Materials: A Simplified Standard Adsorption Method and a Simplified Broekhoff– de Boer Method, Langmuir, 1999, 15, 5403-5409.
[16] Luechinger M., Pirngruber G.D., Lindlar B., Laggner P., Prins R., The effect of the hydrophobicity of aromatic swelling agents on pore size and shape of mesoporous silicas, Micro. Meso. Mater., 2005, 79, 41-52.
[17] Chen Y., Cao Y., Suo Y., Zheng G.P., Guan X.X., Zheng X.C., Mesoporous solid acid catalysts of 12-tungstosilicic acid anchored to SBA-15: Characterization and catalytic properties for esterification of oleic acid with methanol, J. Taiwan Inst. Chem. E., 2015, 51, 186-192.
[18] Brahmkhatri V., Patel A., 12-Tungstophosphoric acid anchored to SBA-15: An efficient, environmentally benign reusable catalysts for biodiesel production by esterification of free fatty acids, Appl. Catal. A: Gen., 2011, 403, 161-172.
[19] Jeenpadiphat S., Björk E.M., Oden M., Tungasmita D.N., Propylsulfonic acid functionalized mesoporous silica catalysts for esterification of fatty acids, J. Mol. Catal. A: Chem., 2015, 410, 253-259.
[20] Pirez C., Caderon J.M., Dacquin J.P., Lee A.F., Wilson K., Tunable KIT-6 Mesoporous Sulfonic Acid Catalysts for Fatty Acid Esterification, ACS Catal., 2012, 2, 1607-1614.